Final Report
Contract No.: ONR N00014-92-J-1868
(ONR N00014-88-K-0317)

Properties of E-beam Interactive Oxide Films for Nanometer Scale Structures

by

R.C. Buchanan
J. Kim

March 1995

This document has been approved for public release and sale; its distribution is unlimited.

Department of Materials Science and Engineering
University of Cincinnati *
498 Rhodes Hall
Cincinnati, OH 45243

This research was supported by DARPA under
Office of Naval Research Sponsorship

Production in whole or in part is permitted for
any purpose of the United States Government

* Grant No. N00014-92-J-1868 was awarded to The Board of Trustees of the University of Illinois, Dr. Buchanan subsequently left the University of Illinois and assumed a position with the University of Cincinnati The final report is being submitted through the University of Illinois

19950601 011

Abstract

E-beam generated ultrastructures in oxide and halide film substrates have been investigated for high density memory and lithographic applications. In order to create the nanometer scale patterns (holes, lines, channels), a dedicated STEM was used and also used for exposure studies, imaging, microdiffraction analysis and for monitoring the transmitted beam. High ionic character, high heat of formation and high melting point were identified as desirable material characteristics by the oxide film studies. Therefore, halide materials were studied in order to evaluate the formation time for its film structures using the e-beam method. Amorphous AlF_3 film was deposited on to substrate at cryogenic temperature. Hole resolution in the sputtered halide films of 5 nm holes on 8.1 nm centers was achieved with exposure times in the millisecond range, 2 ~ 3 orders of magnitude lower than produced by other technique. The generated oxide films for applying high density memory needs the apparatus to read / write using oxide films. This report describes an E-beam addressed, high speed, mass memory system that would be capable of 10^{12}-10^{14} bits with a data transfer rate about 10^6 bits per seconds. The development of the storage medium and the proper electron beam optics system for the mass memory system is a most crucial element of E-beam generated ultrastructures. There are two different types evaluated for attempting the above purpose. One is using the fly's eye lens and the other is using scanning tunneling microscopy unit. Both promise a new read /write system with fast accessing time and are described in detail in this report.

Table of Contents

Accesion For
NTIS CRA&I ☑
DTIC TAB ☐
Unannounced ☐
Justification .....
By A 272848
Distribution /
Availability Codes
Dist | Avail and / or Special
A-1

Properties of E-beam Interactive Oxide Films for Nanometer Scale Structures

R. C. Buchanan
Dept. of Material Science and Engineering
University of Cincinnati , Cincinnati, OH 45221

I. Introduction

The development of a high density and fast access memory system is the ultimate concern for computer applications. With the advent of the magnetic memory systems, which are convenient and of relatively large capacity, the development of other memory systems, including e-beam access memory technology, ceased. However, further progress of computer technology requires extensive and fast access memory systems, beyond the capability of the magnetic memories now in use. Factors that have prevented the development of an alternative memory system include the following: 1) Lack of a suitable high speed, high density target material; 2) Lack of a suitable detecting system having fine spatial resolution; and, 3) Lack of portability, small size and reasonable cost for the systems proposed.

High density memory systems require high density memory elements without loss of information. This limitation can be satisfied by oxide compounds, which are excellent dielectric materials that store electrical information. To take advantage of this capability, it is essential to develop a high spatial resolution technique for reading and writing within a small region.

The barrier is that there is no suitable material to obtain this high spatial resolution. The selective removal of material in highly ionic solids

was first observed in NaCl foils by Broers in 1978[1]. A number of oxide and metal halide compounds when exposed to high intensity electron beam irradiation undergo a rapid loss of constituents permitting lithographic features to be produced on the order of 1~ 20 nm[2, 3]. Structures on this scale are among the smallest currently obtainable in lithographic systems, surpassing the limit imposed by the spatial range of secondary electrons generated in conventional high resolution polymeric materials, such as PMMA[4]. The inherent high resolution characteristics of these materials, as well as a lack of understanding of the exposure process involved, has fueled an interest in further study of inorganic resist materials.

The lithographic characteristics of oxide materials have been observed by Hollenbeck and Buchanan [5,6] to depend on the method of film preparation and on the resulting microstructural characteristics and to prove the formation of nanoscale structure using scanning transmission electron microscope (STEM). The above studies have shown that proper control of film deposition should produce improvements in resist properties, particularly exposure requirements. Substrate characteristics desirable in the high density and fast access applications, in addition to nanometer scale resolution, include low dosage requirements for exposure, high material removal rates, high contrast, good physical and chemical durability and good thermal conductivity.

This report characterizes new halide resist materials capable of nanoscale resolution with a reasonable drilling rates and an E-beam addressed, high speed, mass memory system that would be capable of 10^{12}-10^{14} bits with a data transfer rate about 10^6 bits per second. The development of the storage medium for the mass memory system is a most crucial element of E-beam generated ultrastructures. The proper electron beam optics system

is also essential part of this report. And it also aims on the development of read / write detecting system for nanoscale structure.

II. Experimental Procedure

The thin films were deposited by rf sputtering from dense polycrystalline oxide targets directly onto formvar coated 200 mesh-grids stabilized with SiO. The resulting resist/substrate arrangement is shown in figure 1. The formvar and SiO coatings are amorphous and show no deterioration under exposure conditions. Sputtering parameters were chosen to allow the fabrication of both polycrystalline and amorphous films from 15 ~ 150 nm in thickness. To promote the formation of amorphous films, the substrate temperature was controlled at 77 K through the use of a liquid nitrogen cold stage.

Electron beam exposure of the thin films was carried out using a modified V. G. Microscope HB-5 STEM, capable of producing a 100 keV beam of electrons with a dose rate of 1×10^5 A/cm^2 and a final spot diameter less than 1 nm. Generation of lithographic patterns is being carried out through computer control of the beam deflection and beam blanking systems in the microscope.

III. Results and Discussion

A) Halide materials

In the previous study, the two most important deposition parameters found to influence the microstructure of rf sputtered oxide films were substrate temperature and rf power. Deposition conditions necessary to

promote the formation of uniform amorphous films were also found to be strongly dependent on the material itself. The deposition of films at cryogenic temperature limited diffusion of adatoms on growing films and resulted almost exclusively in amorphous film structures. Limited sputtering power minimized local heating of the film surface during deposition. To avoid local surface heating in films, powers were limited to less than 50 Watts and a 10 min cooling period for every 30 min of deposition time.

In previous report, the resolution of hole and line patterns in Al_2O_3 was studied as a function of film thickness and total exposure dose, using multiple dose / multiple spacing patterns. At optimum film thickness was found to occur at approximately 90 nm where 5.0 nm holes could produced on 8.9 nm centers. Slightly better resolution is reported at exposure doses of 13×10^2 and 4×10^2 C/cm^2, however, holes formed at these doses did not result in complete material removal. Figure 2 shows dot patterns produced in amorphous Al_2O_3 film.

Material properties which were found to correlate well with the exposure response of amorphous oxide films were the bonding character, heat of formation and melting point. A rapid response was found to occur in materials with high ionic character, high heats of formation and high melting points. The highly ionic materials with high bonding strength are required to produce films with sufficient sensitivity to make them viable resists. In order to find more fast removal materials, the halide films was chosen and have been studied.

Direct comparison of evaporated amorphous AlF_3 films with rf sputtered amorphous Al_2O_3 films has shown that the exposure requirements of the two materials are similar, however, there also exists a number of differences in their lithographic response. The end point dose measured in 50

nm thick AlF_3 films was 3.5×10^3 C/cm^2. Figure 3 shows a bright field STEM image of a pattern produced in amorphous. Small crystallites are observed near the newly formed holes, much like those observed in the oxides, and are thought to be aluminum metal. Diffraction patterns were obtained from these particles, but could not be properly identified, however, metal formation in fluorides has been reported by Muray *et al.*[7].

The first difference apparent in the response of AlF_3 is the absence of a well defined jump in the transmitted beam signal. This indicates that the material removal process is somewhat different in this material, the difference likely being associated with the removal of the anion species. The rapid expulsion of oxygen and inert gas in the irradiated region of rf sputtered oxide films does not appear to occur, at least to the same extent, with the fluoride component of AlF_3 films. This may be due to differences in atomic size of the anions (O^{2-} {1.40 Å}, F^- {1.36 Å}), the possible molecular association of oxygen, or the presence of inert gas in rf sputtered oxides. The primary mechanism of material removal in AlF_3 appears to be the loss of anion surface species and displacement of aluminum ions, as supported by the work of Muray[8]. The exposure requirement which has been reported for AlF_3 in this study was determined from the point where no further increase in transmitted signal was found.

Another difference in the lithographic behavior of AlF_3 is the appearance of considerable damage to areas of the film near exposed holes, as seen in Figure 3. To more quantitatively examine this difference and its effect on production of adjacent structures a series of line patterns were produced using 40, 60, 80 and 100 holes per line in both amorphous AlF_3. These line patterns and corresponding transmitted beam traces are shown in Figure 4 . The transmitted beam traces show that each hole was exposed for

approximately 40 ms (4×10^3 C/cm^2). As more holes were used to make each line the spacing was gradually decreased and continuous lines were formed. Damage to nearby material can be seen in both the AlF_3 and Al_2O_3 films. However, the extent of damage in the AlF_3 was found to be much greater. This damage is illustrated by the lighter areas between and adjacent to exposed lines. The transmitted beam signal from the 100 hole/line patterns also shows that the material removal at small hole spacing in Al_2O_3 occurs much the same way as at larger spacing while the signal from the AlF_3 film was found to change significantly. The change in transmitted beam signal at very small hole spacing is believed to support the observation that longer range damage occurs in amorphous AlF_3 and that this damage has a significant and measurable effect on the removal of material in adjacent areas. Although some damage is also observed in amorphous Al_2O_3 it is much smaller in spatial extent. Amorphous Al_2O_3 films, therefore, have better characteristics for the production of line geometries.

Multiple exposures of crossing line patterns in AlF_3 and Al_2O_3 films were also examined and again revealed differences in the lithographic characteristics of these materials. Figures 5 and 6 show crossing line patterns exposed using 100 holes/line and a dose of 2.5×10^2 C/cm^2 per hole. The STEM bright field images of the single exposure (Figures 5(A) and 6(A)) show that material removal has progressed slightly further in Al_2O_3, although both patterns have been clearly formed using an exposure dose of approximately 1/10 that required for a single discrete hole. As the number of exposures is increased to 5, 10, and 20, the pattern stays well defined in AlF_3 and the extent of damage to nearby areas is again quite extensive. Increasing the number of exposures in Al_2O_3 resulted in more severe degradation of the pattern than in AlF_3. This degradation resulted from a greater loss of material in regions

where lines were crossed. The holes produced where lines crossed received the most exposure dose and appeared to grow at the expense of other regions which have been filled in (Figure 6). The extent to which this type of material displacement and redeposition occurs appears to be greater for Al_2O_3 than AlF_3 films. Small crystallites can be seen to form after 10 and 20 exposures of the Al_2O_3 film (Figure 6) and higher magnification images of AlF_3 also revealed the presence of crystallites.

From the direct comparison of amorphous AlF_3 and Al_2O_3 films both similarities and differences in the lithographic characteristics of these materials have been found. Both materials required a dose of approximately 5×10^3 C/cm^2 for complete exposure, however the progression of material removal was found to be different. Transmitted signal traces taken during exposure of AlF_3 indicated material was removed at a fairly uniform rate with no rapid discontinuities, indicating that material is continually lost from the irradiated surfaces until hole formation is complete. Line and crossing line patterns also revealed that the extent damage to nearby areas was greater in AlF_3 films while the problem of material redeposition was more significant in Al_2O_3. The more extensive damage to nearby areas in AlF_3 may indicate a higher sensitivity to lower energy electrons while the rapid displacement of a relatively large amount of material during the exposure of Al_2O_3 is thought to be responsible for material redeposition effects in these films.

B) Memory systems

Interests in electron-beam generated ultra structures stem from their demonstrated potential for high density data storage (mass memory) as well

as to their potential for creating high resolution lithographic masks, molecular sieves, synthesis templates, and light collimators.

The lithographic process available for microfabrication of electronic devices are what currently limits the size of these devices. These type of lithographs include photo, X-ray, E-beam, and ion beam lithography. Electron and ion beams offer the highest resolution lithography available at this time. The ultimate resolution in these systems is set by the range over which the primary beams interact with the resist. In polymeric resist materials this range of interaction is determined by the lateral spreading of the low energy secondary electrons generated within the resist materials. It is these secondary electrons which are responsible for the exposure mechanism of the resists. This limits the ultimate resolution obtainable using PMMA[4] and E-beam exposure to approximately 8-12 nm. Ion optical systems are not presently capable of producing beams with a compatible final spot size.

Figure 2 shows a dot matrix pattern drilled into the amorphous alumina film substrate with densely packed holes and good contrast levels between the drilled and undrilled areas. Each hole is about 5 nm in diameter and the film thickness is 90 nm. At the density shown in Figure 2, the entire 10^{14} bit memory would fit in an area 15 cm square. This would allow the text of a 6 million volume library to fit in the area of one book page.

The existence of a promising memory media focuses attention on the development of a read / write system. In this report two methods will be introduced to obtain the above goal.

1) Fly's eye lens

It is necessary to develop a suitable electron optical design capable of rapidly deflecting electron beams to the 10^{14} bits of the system. This is a difficult problem because the aberrations found in electron optical system

have generally limited the deflection of electron beams to roughly 10^4 spot diameters. This is due to the fact that as the beam is deflected off of the optic axis , the aberrations of the system make the beam diameter larger which resides the bit storage density to a low level for large deflection angles.

Some of this discrepancy can be reduced by designing parallel electron beam systems. Such parallelism id desirable for solution of other system problems. For instance, the proposed memory might be designed to use 100 bit words. In this case, 100 electron beam tubes each capable of storing 10^{12} bits would be required . Such parallelism increases the data transfer rate by a factor of 100. It also greatly increases system reliability since error correcting codes could be used that would allow failure of an E-beam tube with complete recovery of all stored data even though one bit of the word would be missing.

It is unlikely, however, that parallelism alone will give the required resolution. After considerable analysis, a system was found which seems capable of deflecting the beam to between 10^{11} and 10^{12} positions. The primary components are the electron gun, electron beam deflectors, a fly's eye lens array, the target having the memory media, and the electron detector. The heart of this system is a fly's eye lens array that is placed very close to the memory media target plane. Figure 7 shows a schematic diagram of this system. Each of these small lenses is used to focus the beam on a small array of bits in the memory media. For instance, for a 10^{12} bit tube, each lens could focus to an array of 10 by 10 =10 bits. A array of 10^3 by 10^3 =10^6 lenses, each focusing to 10 bits will result in $10^6 x 10^6 = 10^{12}$ bits.

In principle electron beams should be able to fabricate structures with dimensions on the order of the beam diameter. Advances in field emission electron sources and E-beam optics has produced STEMs which are capable of a spot size of less than 0.5 nm. Development of resist materials sensitive only

to high energy primary electrons, and not lower energy secondary electrons is, however, necessary to fully utilize the resolution of such a system. A major advantage of electrons is that they are very easy to deflect rapidly by electronic means, and indeed, electron microscopes are available that deflect the electron beam across 5 cm in less than a nanosecond. An electron beam deflection system, therefore, have more than a 10^6 times speed advantage over other technologies.

2) STM unit

The development of the Scanning Tunneling Microscopy (STM) provides the possibility for a new optical system having high spatial resolution (1 Å). This research proposes a new method for obtaining the high density ($10^{11}/cm^2$), fast access times (less than 1 nsec) by use of an e-beam addressed memory and detecting system (applying voltage is less than 1 keV) and an advanced target material for storing the information.

A brief procedure for preparation of the target memory substrate is as follows:

1) A Si substrate, having highly doped n-type Si (1 Ω-cm) on lightly doped p-type Si (400 Ω-cm), is prepared, 2) Amorphous Al is deposited by sputtering methods at cryogenic temperatures, 3) Electrochemical etching is applied to obtain regular hole structures and the Al is changed to Al_2O_3 during this procedure, 4) SiO_2 in the hole regions is developed through oxidation, and finally 5) Al is redeposited with biased angle on the thin film. These processing steps are illustrated in Figure 8.

Figures 9 and 10 show the mechanism for holding electrical information in a sample and electrical circuit system respectively. Accelerating electrons (1 keV) produce electron and hole pairs in SiO_2. The electrons have high mobility in SiO_2 and move out. However, holes are confined in the interface

between SiO_2 and Si. This causes the applied bias voltage (40 V) to produce an intense local field at the interface SiO_2 and Si. When the voltage is removed, the immobile positive charge remains at the interface. The cylindrically applied aluminum around the target holes results in a common deflector function and enables focusing of the e-beam. An optic system and gun design by the IBM research group can be a possible alternative to this writing procedure. To read data nondestructively, no voltage is applied between the Al and n-type Si and a lower current electron beam is applied between the Al and p-type Si. This causes excess holes to diffuse to the p-n junction. For data readings of zero, electron hole pairs created by the electron beam are recombined and no electron current is detected. In this procedure, there is no consumption of holes. Therefore, the reading operation is continuously possible. The capacitance of the p-n junction of the memory is very small because of the high resistivity of the p-type Si and by the use of high bias voltage. This, coupled with the excellent gain of the readout process allows for very high readout frequencies. Data is erased from storage by performing a destructive read out operation, i.e., application of a negative voltage across the aluminum and the n-type silicon layer. In this procedure, holes at the interface are recombined with electrons.

The nanoscale alumina structure contains periodic uniform pores (20~50 nm), in which the pore density can reach as high as $10^{11}/cm^2$. The access time is limited by the actuator movement speed but a parallel alignment of the STM unit can multiply the speed by more than 1 Gbits/sec. This material is thermally very stable, has high dielectric constant and has good resistance to heavy element deposition. Material preparation is easy and mass production is also easily achieved. These properties make it possible to provide other technically important procedures: 1) Deposition of metal and

semiconductor materials, 2) Pattern transfer techniques, 3) Mask for direct writing, and 4) Ion implantation masks. In pursuing the above goals, collaborative efforts (Electronic and Systems Designs Group at the University of Cincinnati) will be explored in analysis of the circuit design and testing systems for target analyzation and the development of a multi-tip STM unit. Additionally, a new tip and micro optic design for an STM unit at IBM enhances the chance for nanoscale lithography technology using our material as a targeting system without the Al redeposition process. Their tip can be also be applied to electron sources for memory systems. The Further development of this material has enormous possibility for the advent of new nanoscale lithography and an ultimate memory system.

IV. Conclusions

1. Evaluation of amorphous AlF_3 and Al_2O_3 films under identical exposure conditions revealed similar dose requirements and amorphous Al_2O_3 films showed superior characteristics for exposure line patterns.
2. The exposure process of amorphous AlF_3 films was found to be different compared to amorphous Al_2O_3 films due to the ionic size difference.
3. Using the fly's eye lens, the aberration effect can be overcome.
4. It is possible to obtain a simple read / write system using STM unit.

V. Acknowledgments

We thank the staffs of Materials Research Labs for the use of the equipment pertaining to this experiment. This work was supported by

DARPA under Office of Naval Research contracts No. N00014-88-K-0317 and N0014-92-J-1868.

VI. Reference

1. A. N. Broers J. Cuomo J. Harper W. Molzen R. Laibowitz and M. Pomerants, "High Resolution Electron Beam Fabrication Using STEM," *9th International Congress on Electron Microscopy*, III 343-354 (1978).

2. D. C. Joy, "The Spatial Resolution Limit of Electron Lithography," *Microelectronic Eng.*, 1 103-19 (1983).

3. E. Kratschmer and M. Issacson, "Nanostructure Fabrication in Metals, Insulators, and Semiconductors Using Self-Developing Metal Inorganic Resists," *J. Vac. Sci. Technol.*, B4 361-4 (1986).

4. M. Issacson and A. Murray, "In Situ Vaporization of Very Low Molecular Weight Resists Using 1/2 nm Diameter Electron Beams," *J. Vac. Sci. Technol*, 19 [4] 1117-20 (1981).

5. J. L. Hollenbeck and R. C. Buchanan, "Properties of E-Beam Interactive Oxide Films," *Mat. Res. Soc. Symp.*, 72 289-294 (1986).

6. J. L. Hollenbeck and R. C. Buchanan, "Nanometer-Scale Structures Produced in Oxide Films," *Proceedings of the 45th Annual Meeting of the Electron Microscopy Society of America*, 396-7 (1987).

7. A. Murray, M. Isaacson and I. Adesida, "AlF_3 - A New Very High Resolution Electron Beam Resist," *Appl. Phys. Lett*, 45, 589-591 (1984).

8. A. Murray, Ph. D. Thesis, Cornell University, (1985).

VII. List of Figures

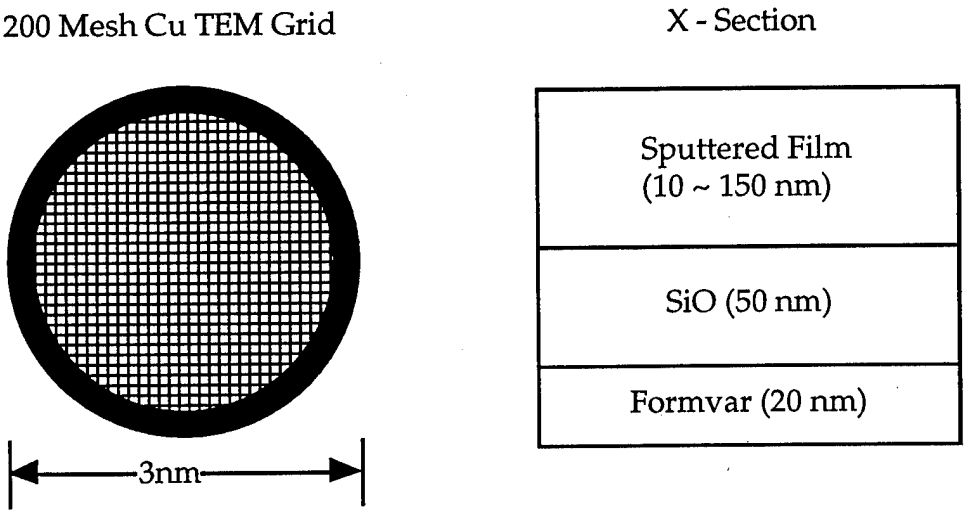

Figure 1. Schematic illustration of the 200 mesh coated copper grid used as a support substrate for rf sputtered films.

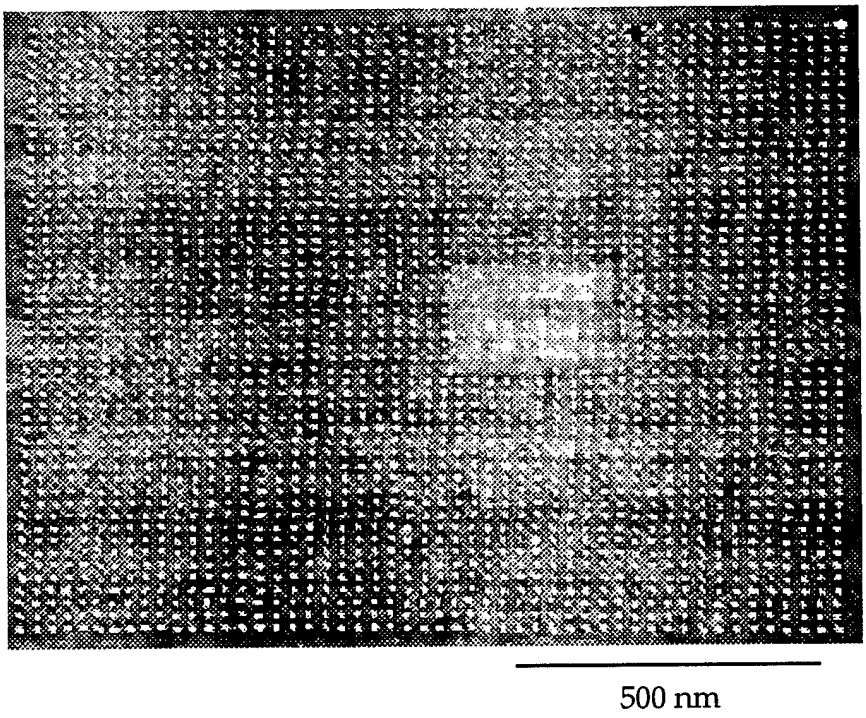

Figure 2. Dot patterns produced in amorphous Al_2O_3 film.

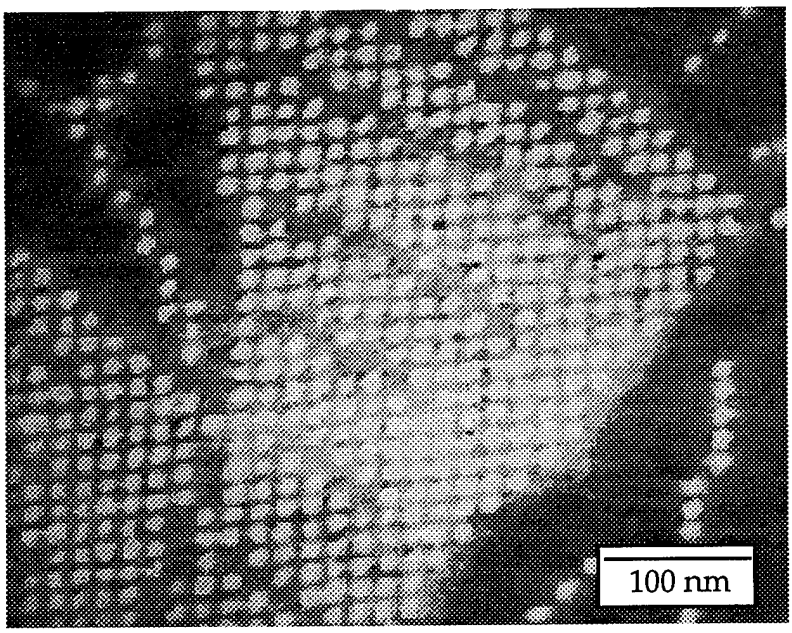

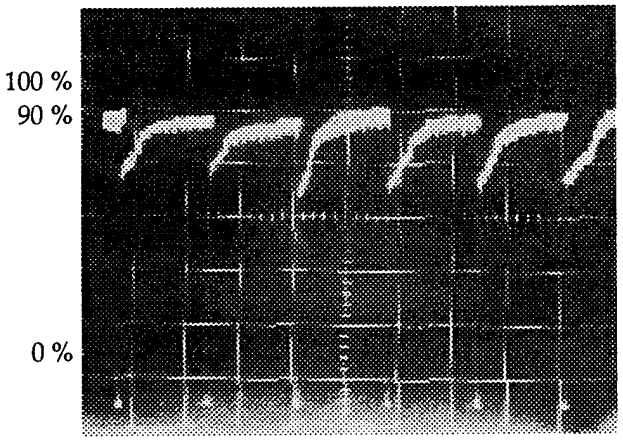

(x-axis: 100 ms/div.)

Figure 3. STEM bright field image of pattern produced in an evaporated AlF_3 film and a typical transmitted beam trace during exposure.

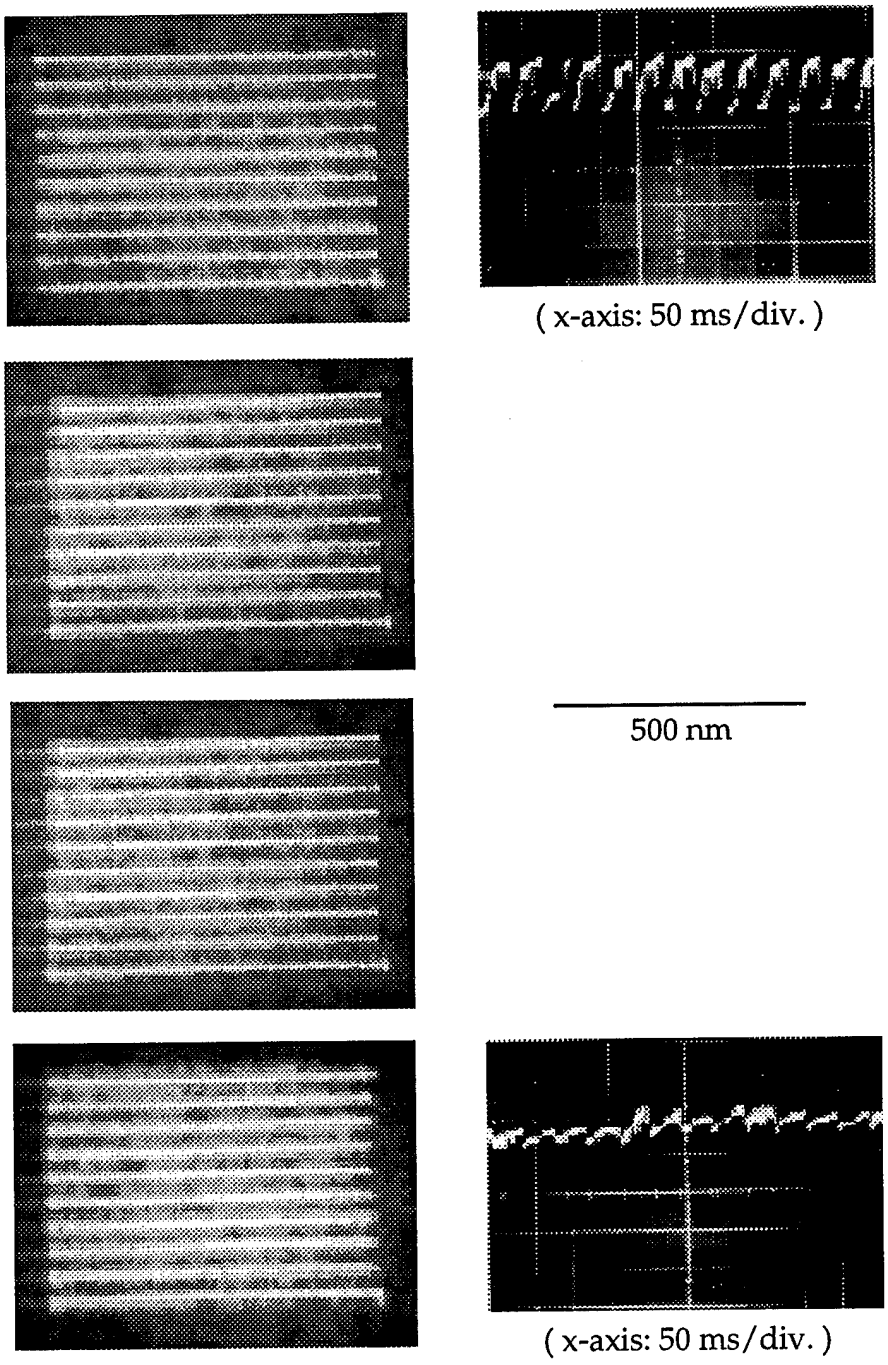

Figure 4. Line patterns produced in amorphous AlF_3 using 40, 60, 80 and 100 holes / line and the transmitted beam signal from the exposure of 40 and 100 hole / line patterns.

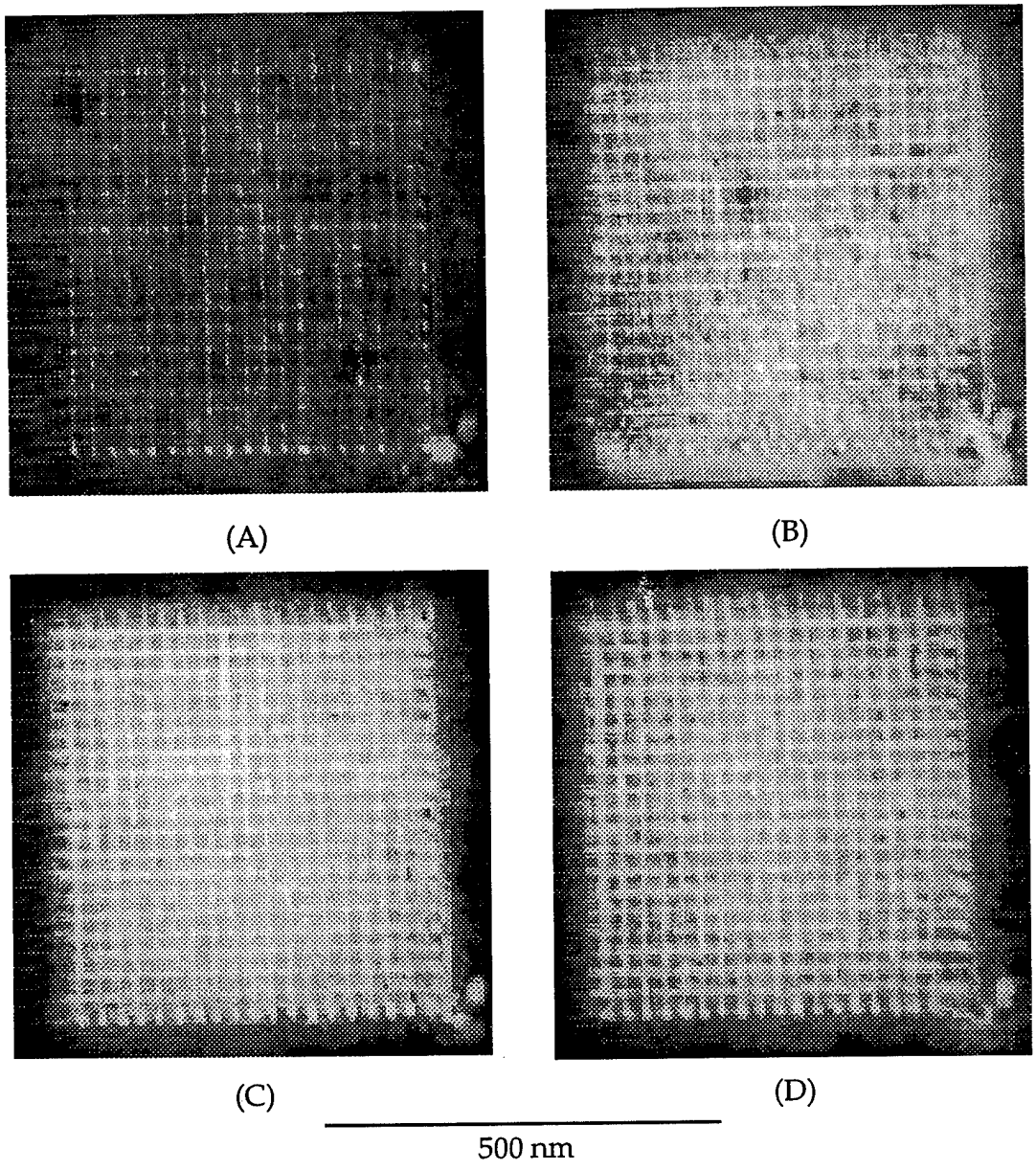

Figure 5. Crossing line pattern produced in an amorphous AlF_3 film using 100 holes per line and multiple exposures (2.5×10^2 C/cm^2 per line): (A) 1 exposure, (B) 5 exposures, (C) 10 exposures and (D) 20 exposures

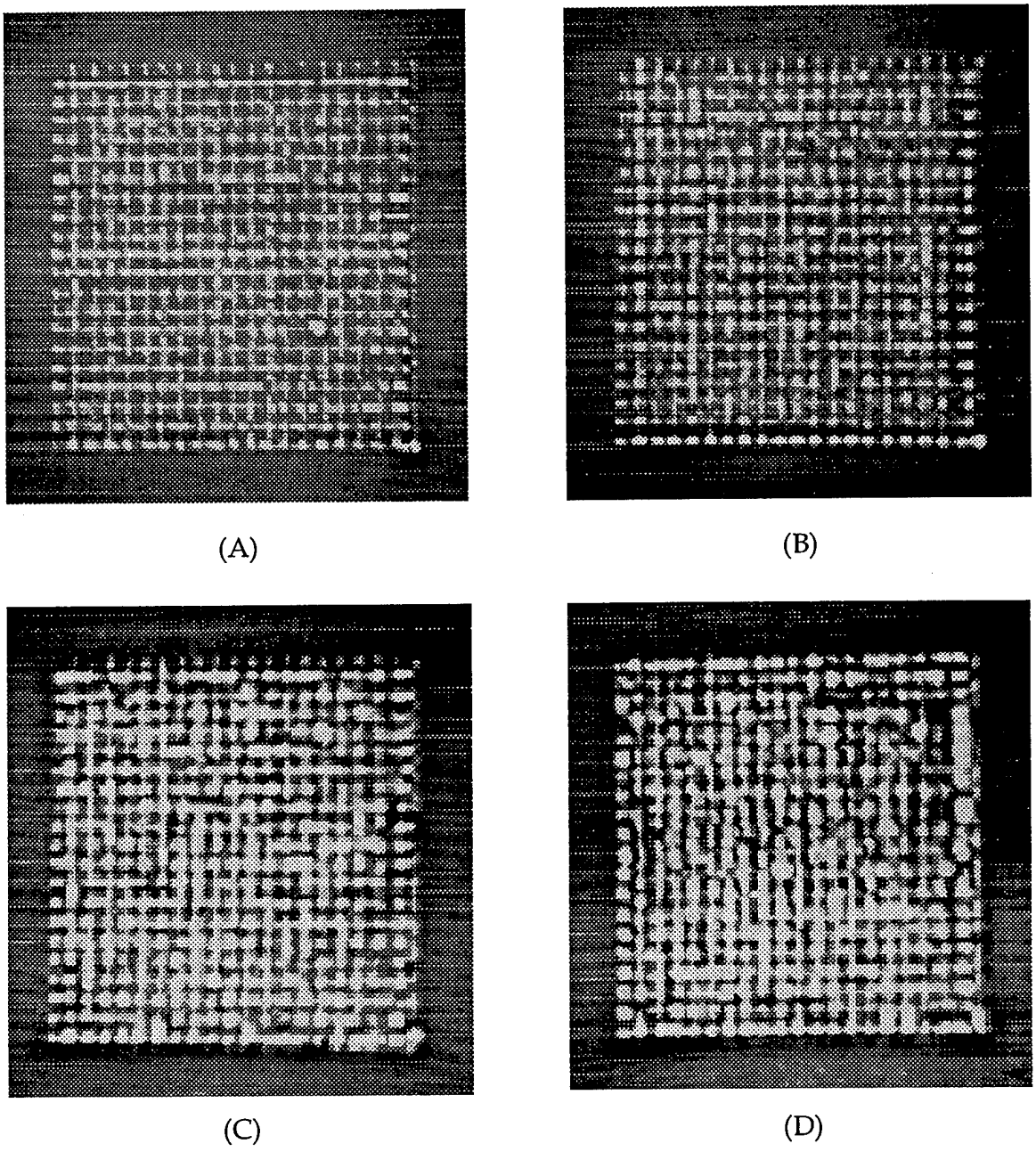

Figure 6. Crossing line pattern produced in an amorphous Al_2O_3 film using 100 holes per line and multiple exposures (2.5×10^2 C/cm^2 per line): (A) 1 exposure, (B) 5 exposures, (C) 10 exposures and (D) 20 exposures

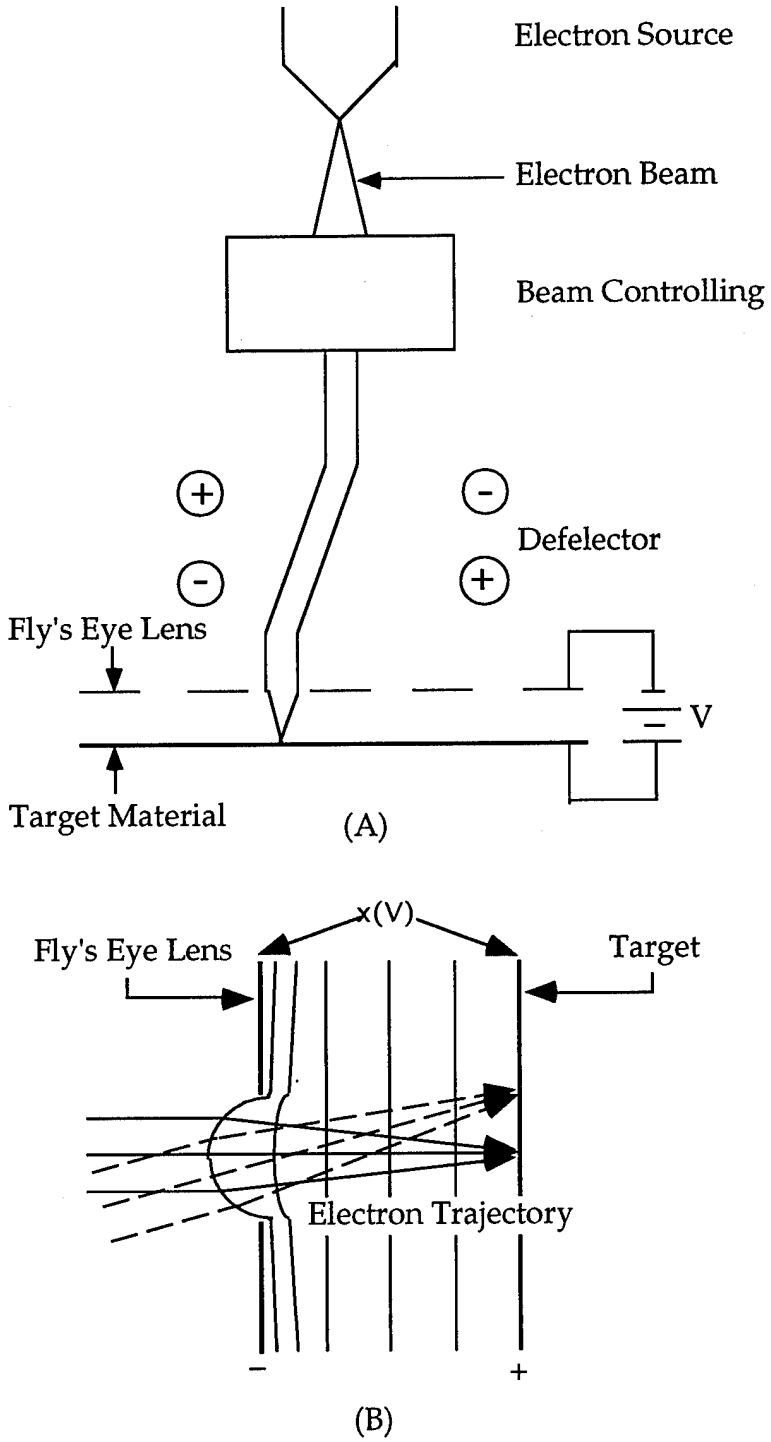

Figure 7. Schematic diagram of a optical design for the high density memory system (A) deflecting system (B) fly's eye lens

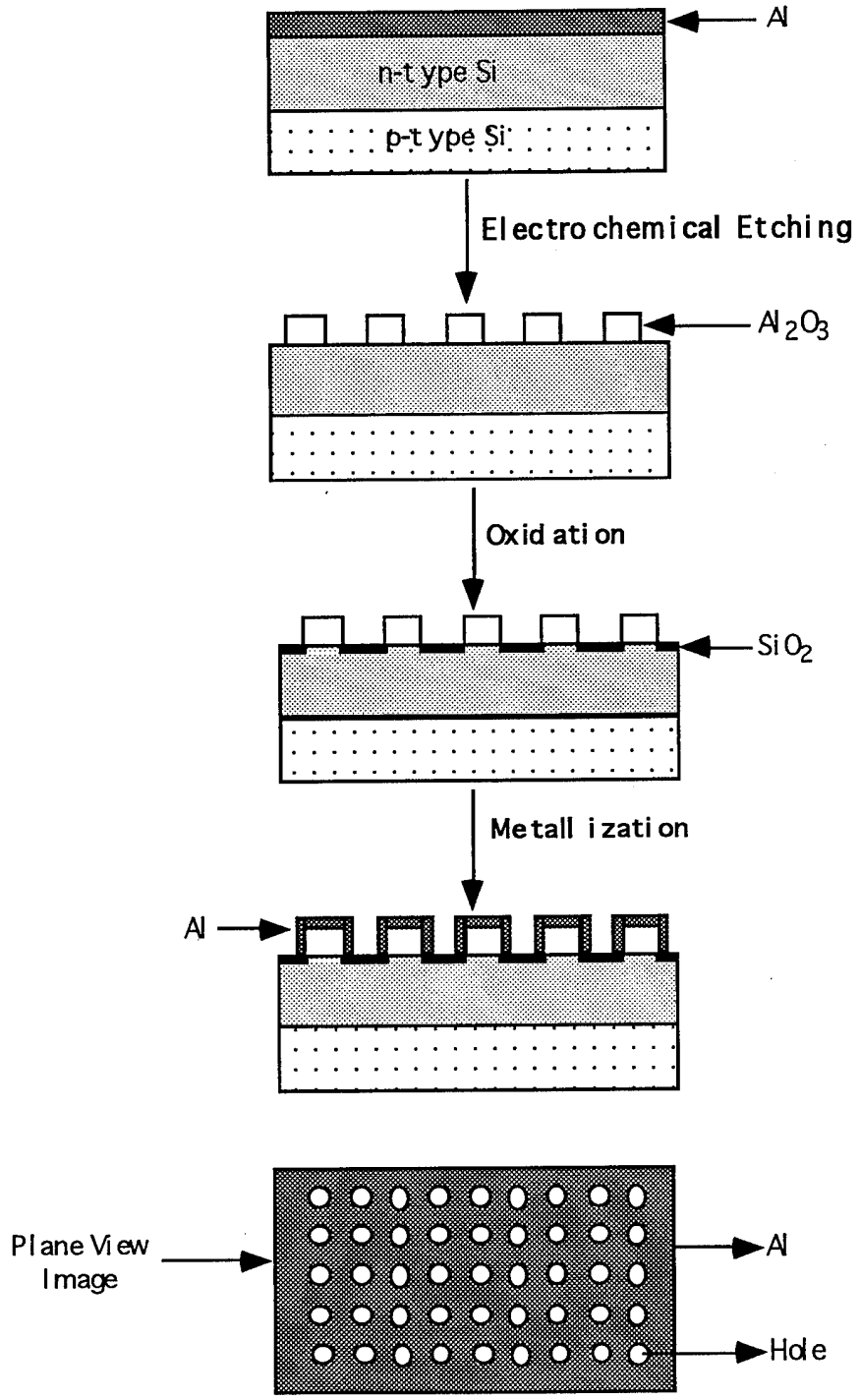

Figure 8. Sample preparation of high density memory system

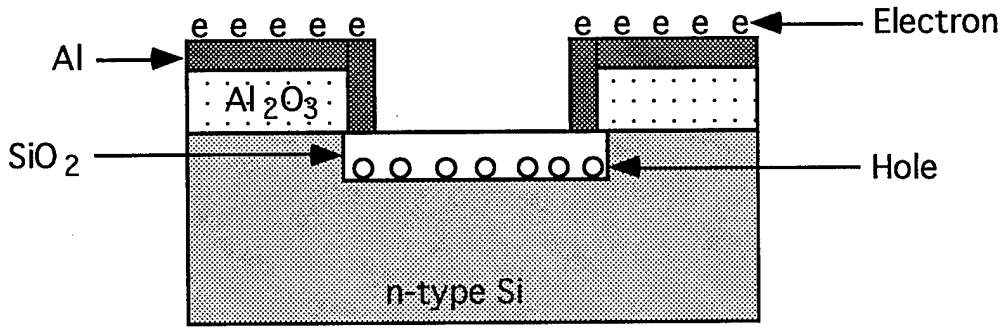

Figure 9. Electron and hole state after voltage applied to the sample. Elctrons go out due to high mobility and hole is trapped between oxide and silicon interfaces.

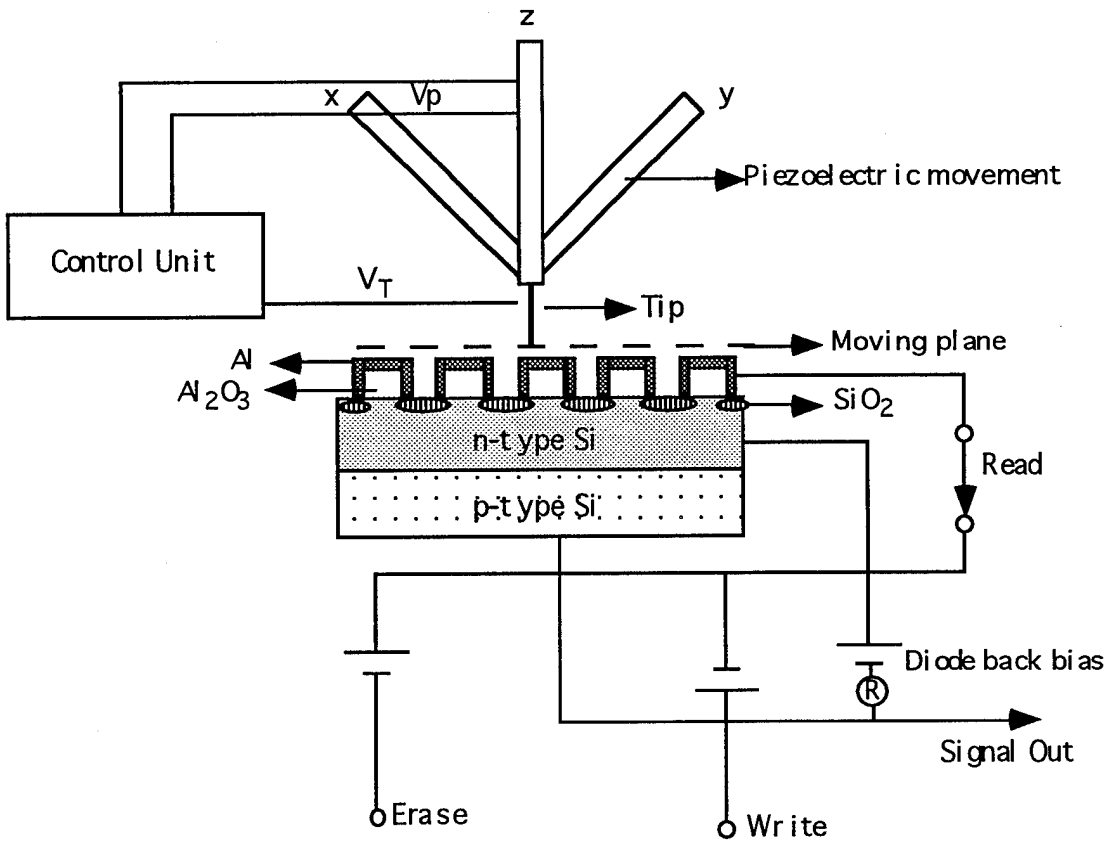

Figure 10. Schematic diagram of memory system using STM unit